Am J Transl Res 2020;12(9):4902-4922
www.ajtr.org /ISSN:1943-8141/AJTR0110985

Original Article

Chaiqi decoction ameliorates vascular endothelial injury in metabolic syndrome by upregulating autophagy

Xun Chen[1,2*], Xiao-Ru Yan[3*], Jing Liu[2,4], Li-Ping Zhang[2,4]

[1]Xiyuan Hospital, China Academy of Chinese Medical Sciences, Beijing, China; [2]Beijing University of Chinese Medicine, [3]Guang'anmen Hospital, China Academy of Chinese Medical Sciences, Beijing, China; [4]Dongfang Hospital of Beijing University of Chinese Medicine, Beijing, China. [*]Equal contributors and co-first authors.

Received March 17, 2020; Accepted July 15, 2020; Epub September 15, 2020; Published September 30, 2020

Abstract: Objective: The present study aimed to investigate the protective effect of the Chaiqi decoction on vascular endothelial injury in metabolic syndrome and to determine whether the underlying mechanism was associated with autophagy. Methods: Chaiqi formula granules were administered to a rat model of metabolic syndrome established by feeding with a high-salt-sugar-fat diet (HSSFD). The drug-containing serum was used in a hyperglycemia cell model established using HUVECs cultured with palmitic acid PA. The influence of the Chaiqi decoction on metabolic syndrome-related vascular endothelial injury and autophagy was investigated. Autophagy flux was assessed *in vitro* by transfecting cells with GFP-mRFP-LC3 adenoviruses or incubating with DALGreen and DAPRed. Results: The metabolic syndrome model rats displayed adiposity, hyperglycemia, dyslipidemia, hypertension, thickened intima, deposition of various forms of collagen and lipid droplets, downregulated levels of phosphorylated endothelial nitric oxide synthase and nitric oxide, upregulated expression of endothelin 1, and dysfunctional autophagy. All these abnormalities were ameliorated by administration of the Chaiqi decoction to the metabolic syndrome rats. Furthermore, the Chaiqi-containing serum could upregulate autophagy similarly to rapamycin, in a time-dependent manner. Conclusion: The Chaiqi decoction could ameliorate vascular endothelial injury by improving autophagy in metabolic syndrome.

Keywords: Metabolic syndrome, Chaiqi decoction, vascular endothelial injury, autophagy

Introduction

Metabolic syndrome, one of the major risk factors for cardiovascular disease (CVD), refers to a group of metabolic disorders that include symptoms of adiposity, hyperglycemia, dyslipidemia, and hypertension [1]. The incidence of metabolic syndrome has been growing rapidly over the last decades, and is associated with a two-fold increase in the incidence of CVD [2, 3]. Unfortunately, CVD is a primary cause of mortality worldwide [4]. Vascular endothelial dysfunction, an early event in the development of CVD [5], is often accompanied by progression of metabolic syndrome [6]. In metabolic syndrome, the decreased synthesis of nitric oxide (NO) and notably increased Endothelin-1 (ET-1) levels indicate vascular endothelial dysfunction [7, 8]. There is no effective treatment for metabolic syndrome; therefore, improvement of vascular endothelial dysfunction has become a promising therapeutic strategy to reverse CVD.

ET-1 is a 21 amino acid-long endogenous vasoconstrictor peptide, which is mainly produced and released in vascular endothelial cells [9]. Under normal physiological conditions, ET-1 binding with endothelin receptor A (ETA) stimulates vasoconstriction, while binding to endothelin receptor B (ETB) causes vasodilation. Increased ETA and decreased ETB levels lead to severe vasoconstriction in pathological conditions [10-12]. Many studies have shown that ET-1 levels in patients with metabolic syndrome are higher compared with those in patients without metabolic syndrome, and is associated with an increased risk of CVD [13, 14]. Samsamshariat et al., in a cross-sectional study including 76 participants, reported that ET-1 was not only increased in patients with metabolic syndrome, but also suggested that it is a risk factor for developing endothelial dysfunction [8]. NO, an important vascular signaling molecule, plays a crucial role in regulating vascular function. NO is synthesized from

L-arginine by endothelial-nitric oxide synthase (eNOS) generating NO and L-citrulline in endothelial cells, and then spreads to the smooth muscle cells, stimulating them to produce cyclic (c)GMP and inducing the relaxation of vessels [15, 16]. Thus, reduced bioavailability and synthesis of NO promotes the endothelial dysfunction that is commonly associated with CVD and type 2 diabetes mellitus [17, 18]. Cui et al. demonstrated that endothelial dysfunction with impaired NO production and eNOS phosphorylation was involved in the progression of metabolic syndrome, while endothelial dysfunction was ameliorated after restoring NO production and eNOS phosphorylation in metabolic syndrome rats [7]. In the present study, we used ET-1 and NO combined with histological examination of the thoracic aorta as indicators of vascular endothelial injury.

Autophagy is a self-protective process that not only regenerates and releases amino acids, lipids, and other metabolic precursors to maintain cellular homeostasis, but also participates in the development of a variety of diseases, such as metabolic syndrome and CVD [19, 20]. Under nutrient excess conditions, autophagy in CVD tends to be suppressed because of excessive activation of mechanistic target of rapamycin (mTOR) [21, 22], which is a negative regulator of autophagy. In the cardiovascular system, the accumulation of degraded metabolites caused by defective autophagy leads to inflammation, apoptosis, and vascular endothelial dysfunction [22-25]. Thus, there is strong evidence for a causal relationship between autophagy and the vascular endothelial dysfunction observed in metabolic syndrome.

Traditional Chinese medicine (TCM) plays an important role in metabolic syndrome treatment and its effects are under investigation. Chaiqi decoction (Chaiqi), a TCM formula, is based on the following treatment principles: “strengthen the spleen and soothe the liver”. Chaiqi is widely used to treat metabolic syndrome in China and has been shown to have therapeutic effects [26]. Previous studies have reported that Chaiqi (5.67 g/kg/day to rats, in distilled water) not only regulates adiposity, hyperglycemia, dyslipidemia, hypertension, and other metabolic disorders [27, 28], but also improves vascular endothelial dysfunction via the nuclear factor kappa B (NF-κB) signaling pathway [29]. Moreover, the NF-κB signaling pathway can interact with mTOR to regulate autophagy [30, 31]. Therefore, the present study aimed to explore the mechanism of action of Chaiqi in improving metabolic syndrome-related vascular endothelial injury through *in vivo* and *in vitro* experiments. The results showed that Chaiqi could alleviate metabolic syndrome-related vascular endothelial injury via activation of autophagy. This finding indicated that Chaiqi could be a potential treatment for vascular endothelial injury in metabolic syndrome.

Methods

Chaiqi decoction preparation and materials

Chaiqi formula granules, purchased from China Resources Sanjiu Pharmaceutical Co. Ltd (Beijing, China), comprised six commonly used herbs: 10 g *Bupleurum* (Certificate of quality number PFC-2018005651), 30 g of *Astragalus membranaceus* (Certificate of quality number PFC-2018005554), 10 g of *Citrus aurantiumL* (Certificate of quality number PFC-20180051-50), 10 g of Atractylodes *lancea* (Thunb.) DC rhizome (Certificate of quality number PFC-2018005335), and 3 g of *Panax notoginseng* (Certificate of quality number PFC-20180054-73). The high-salt-sugar-fat diet (HSSFD, Certificate of quality number 11002900102121; 50% basal feed, 10% lard, 10% egg yolk powder, 2% cholesterol, 7.5% milk powder, 10% fructose, 5% Palmitic acid, 3% salt, 2% fish meal, 0.5% bile salts) was purchased from Beijing KEAO XIELI FEED Co. Ltd (Beijing, China; SCXK 2014-0010). Rapamycin (catalog no. A8167) was purchased from Apexbio (Boston, MA, USA). Pentobarbital (catalog no. P3636) and Palmitic acid (PA; catalog no. P0500) were purchased from Sigma (St. Louis, MO, USA). D-glucose (catalog no. 8150), bovine serum albumin (BSA), Free Fatty Acids (catalog no. A8850), and Dimethyl sulfoxide (catalog no. D8371) were purchased from Solarbio Life Science (Beijing, China). Antibodies recognizing LC3B (Long-chain base protein 3; catalog no. 12741), and beta-actin (catalog no. 4970); anti-rabbit IgG (catalog no. 4412); and 4’,6-diamidino-2-phenylindole (DAPI) (catalog no. 8961) were purchased from Cell Signaling Technology (Danvers, MA, USA). Antibodies recognizing P62 (sequestome 1 (SQSTM1) cat-

alog no. ab109012), Beclin 1 (catalog no. ab207612), ET-1 (catalog no. ab117757), eNOS (catalog no. ab199956), and Goat Anti-Rabbit IgG H&L (catalog no. ab97051) were purchased from Abcam (Cambridge, UK). Antibodies recognizing phosphorylated (Ser1177) eNOS (catalog no. 11156-1) were purchased from SAB Signalway Antibody (Waltham, MA, USA). Human umbilical vein endothelial cells (HUVECs, catalog no. 8000), endothelial cell medium (ECM; catalog no. 1001), trypsin neutralization solution (TNS; catalog no. 0113), 0.25% EDTA (catalog no. 0103), fetal bovine serum (FBS, catalog no. 0500), Dulbecco's Phosphate Buffered Saline (DPBS, catalog no. 0303) were purchased from ScienCell Research Laboratories (Carlsbad, CA, USA). The enzyme-linked immunosorbent assay (ELISA) kits for ET-1 (catalog no. DET100) and NO (catalog no. KGE001) were purchased from R&D Systems (Minneapolis, MN, USA). Cell Counting Kit 8 (CCK-8, catalog no. HY-K0301), DALGreen (catalog no. D675), DAPRed (catalog no. D677i) were purchased from Dojindo Molecular Technologies (Kumamoto, Japan). GFP-mRFP-LC3 (green fluorescent protein-monomeric red fluorescent protein-microtubule associated protein 1 light chain 3 alpha) adenovirus (catalog no. AP19061002) was purchased from Hanheng Biotechnology (Shanghai, China).

Animals

The specific pathogen-free (SPF) grade Sprague-Dawley (SD) rats (n = 53, weighing 200 ± 10 g, 6 to 8-week-old, male) were obtained from Vital River Laboratory Animal Technology, Beijing, China (SCXK 2016-0006) and raised in an SPF animal room at the Research Institute of Dongfang Hospital (Beijing, China; Certificate number SYXK2019-0013), which has a temperature of 23-25°C, humidity of 55 ± 10%, and a light controlled environment (12-h light/dark cycle), with *ad libitum* access to rodent feed and water. The experimental protocol was approved by the Animal Welfare Committee of Dongfang Hospital (Beijing, China; Certificate number 201902). After adaptive feeding for 1 week, the rats were randomly divided into a control group (n = 14) and model group (n = 39) for 8 weeks of intervention. The control group was fed with basic food, while the model group was fed with the HSSFD. All rats had free access to tap water. The rats were weighed once a week. After 8 weeks of intervention, seven rats were randomly selected from each group and anesthetized using 1% pentobarbital (40 mg/kg) via intraperitoneal injection. We evaluated the success of establishing an animal model of vascular endothelial injury in metabolic syndrome by measuring their weight, Lee's index, body fat rate, systolic blood pressure (SBP), blood glucose, serum lipid level, serum ET-1 and NO levels; and the results of hematoxylin and eosin (HE) staining, Masson staining, and Oil Red O staining of the thoracic aorta. Finally, 28 rats from the model group (4 rats were eliminated: 2 for underweight and 2 for asphyxiation during blood pressure measurement) were randomly divided into four subgroups: The model group (n = 7), the normal diet group (ND group, n = 7), the ND+rapamycin (Rapa) group (n = 7), and the ND+Chaiqi group (n = 7), so that we could evaluate the effects of diet control and rapamycin or Chaiqi decoction on vascular endothelial injury in metabolic syndrome. Intervention for 8 weeks comprised: Control group (n = 7), ND group, ND+Rapa group, ND+Chaiqi group fed with the basic diet, while the Model group received HSSFD. Rats in the Control group, Model group, and ND group were treated by intragastric administration of distilled water. Rats in the ND+Rapa group and ND+Chaiqi group were treated with rapamycin (1 mg/kg/day, in distilled water) [32] and Chaiqi (5.67 g/kg/day, in distilled water) [27-29], respectively. The rats were weighed once a week, and their body length (naso-anal lengths) and the fat of epididymis and kidneys were determined at the end of 8 weeks and 16 weeks. To evaluate the degree of obesity of the rats, Lee's index was calculated as (weight (g)^(1/3))/body length (cm) [33]. The body fat rate was calculated as the fat of epididymis and kidneys (g)/weight (g) × 100%.

Preparation of drug-containing serum of rats

SPF SD male rats (n = 18) were randomly divided into six groups (3 d control group, 3 d Chaiqi group, 5 d control group, 5 d Chaiqi group, 7 d control group, and 7 d Chaiqi group). The rats in the control group were treated by intragastric administration of distilled water, while the rats in the Chaiqi group were treated with Chaiqi (5.67 g/kg/day, in distilled water) [27-29]. After 3, 5, and 7 d, all groups were anesthetized.

Blood samples from the six groups were collected separately and sterilely through the abdominal aorta a 2 h after the last drug administration. After settling for a while at room temperature, the drug-containing serum and control serum were separated by centrifugation at 3000 rpm at 4°C for 15 min and then inactivated at 56°C for 30 min. Finally, the drug-containing serum and control serum were stored at -80°C after filtration through a 0.22-μm filter to remove bacteria. Thereafter, the drug-containing serum was diluted with ECM to of 5%, 10%, 15%, 20%, and 30% when different concentrations were required. The best intervention conditions of the Chaiqi drug-containing serum were screened using the CCK8 assay.

Cell culture

HUVECs were grown in ECM containing 5% FBS, 1% ECGs, and 1% Penicillin-Streptomycin. For hyperglycemic conditions, a proportion of the HUVECs was grown and passaged in ECM supplemented with D-glucose to a final concentration of 25 mM (passage 3-4) according to a previously published protocol [25]. Normoglycemic HUVECs were used as the Control group. When hyperglycemic HUVECs were 70% confluent, cells were pretreated with PA (3:1 PA: BSA ratio; PA: 0.4 mM) for 6 h as the Model group. BSA was used to both stabilize the insoluble fatty acids and transport them to the cell. A proportion of the cells was then exposed to either ECM, rapamycin-ECM (Rapa: 10 μM) or Chaiqi-containing serum-ECM for 24 h (according to the results of CCK8) as the ND group, ND+Rapa group, ND+Chaiqi group, respectively. We wanted to evaluate the effects of nutrient control and rapamycin or Chaiqi drug-containing serum on vascular endothelial injury in metabolic syndrome.

Blood biochemical assay

At the end of week 8 and week 16, rats were fasted overnight and anesthetized using 1% pentobarbital (40 mg/kg, administered intraperitoneally). Blood samples were collected separately and sterilely through the abdominal aorta and centrifuged at 3000 rpm for 15 min to obtain serum for subsequent assays. The levels of blood glucose, total cholesterol, triglyceride, high density lipoprotein, and low density lipoprotein were measured using an automatic biochemical analyzer (JAPAN. HITACHI, Tokyo, Japan, 7180).

Systolic blood pressure (SBP)

The SBP of rats in all groups was measured at 8 and 16 weeks of the intervention period, respectively. SBP was determined using the non-invasive tail-cuff plethysmography method and recorded using an automatic sphygmotonography instrument (BP-98A, Softron, Beijing, China).

Detection of ET-1 and NO levels

The cell culture supernatants were collected by centrifugation at 3000 rpm, at 4°C for 5 min, and stored at -80°C. Blood samples were collected as mentioned above. The ET-1 and NO levels were determined using commercially available ELISA kits according to the protocols provided by manufacturers.

Histological examination

About 0.5 cm of thoracic aorta tissue was fixed in 4% paraformaldehyde sectioned, and the tissue sections were subjected to HE staining, Masson staining, and Oil Red O staining. We examined the slides under a light microscope (200 ×, 400 ×; Olympus IX71, Olympus, Tokyo, Japan). Three sections were selected and measured from each group. We then calculated intima thickness, collagen volume fraction (collagen area/total area × 100%), and lipid volume fraction (Lipid area/total area × 100%).

Transmission electron microscopy (TEM)

About 1 mm^3 of thoracic aorta tissue or 1×10^7 cells were fixed in glutaral+osmium tetrachloride. The samples were then dehydrated with acetone solution, followed by embedding and semi-thin sectioning. Complex dyes (0.25% sodium borate: 0.5% basic fuchsin 1:1) were used for staining. After images were acquired under a microscope, ultrathin sectioning was carried out and the sections were placed on thin membrane copper grids prepared with 0.45% Fonnvar solution. Uranyl acete staining and lead staining were then carried out at room temperature. The grids were dried using filter paper and then observed using TEM (TECNAI G2 SPIRIT, FEI, Holland).

Assess autophagic flux

To assess autophagy flux after different interventions, a GFP-mRFP-LC3 adenovirus was

transfected into cultured HUVECs for 5 h at a multiplicity of infection (MOI) of 100. The GFP-mRFP-LC3 protein shows both red (mRFP) and green (GFP) fluorescence at neutral pH. It can form yellow (red+green) puncta that represent autophagosome formation. When an autophagosome fuses with a lysosome, the GFP is degraded because it is pH-labile, whereas mRFP-LC3 (Red puncta in merge pictures) is maintained in the puncta, which then represents the autolysosomes [34]. The relative ratio of red-only versus yellow puncta is us ed as an index of autophagy flux. Signals were visualized under a confocal laser-scanning microscope (Olympus FV1000). Images were acquired using FV10-ASW3.0 software (Olympus).

To assess autophagy flux of Chaiqi drug-containing serum dynamically, after intervention, cells were incubated with DALGreen and DAPRed in the culture medium for 1 h at 37°C. Green (DALGreen) represents the autolysosomes and Red (DAPRed) represents autophagosomes and autolysosomes [35]. The fluorescence images were collected under a fluorescence microscope (Olympus IX71).

Immunofluorescence (IF)

Fresh thoracic aorta tissue was fixed in cold 4% formaldehyde and immersed overnight in buffer containing 30% sucrose. Tissues were then paraffin-embedded and stored until use. Sections were cut at 4 μm, adhered to charged slides, dewaxed with xylene, and hydrated using an ethanol gradient. After rinsing, sections were washed three times in phosphate-buffered saline (PBS) for 5 min, followed by antigen retrieval. After excess fluid was removed, the sections were incubated overnight at 4°C with anti-LC3B antibodies (1:100, Cell Signal Technology). After several washes with PBS, the sections were incubated with Cy3-conjugated rabbit anti-IgG for 60 min at room temperature and then counterstained with DAPI. Signals were visualized on a confocal laser-scanning microscope (Olympus FV1000). Images were acquired using the FV10-ASW3.0 software. Image analysis was performed using computerized densitometry in Image J (Media Cybernetics Inc., Bethesda, MD, USA).

CCK-8 assay of cell activity

Both normoglycemic and hyperglycemic cells were incubated in 96-well plates for 24 h. The cell density was 1×10^4 cells/well before incubation. The Chaiqi drug-containing serum and the blank serum was diluted with ECM to a concentration of 5%, 10%, 15%, 20%, and 30%. In the experiment, normoglycemic cells were exposed to ECM as the control group. ECM without cells was used as a blank group. Hyperglycemic cells pretreated with PA (0.4 μm) for 6 h were exposed to different concentrations of Chaiqi-containing or blank serum for 24, 48, and 72 h as experimental groups. Each group had three duplicate wells. The CCK-8 reagent was added to every well according to the manufacturer's instructions and incubated for 2 h. The cell activity rate was calculated as the optical density ((OD) value of the experimental well-the OD value of a blank well)/(OD value of contrast well-OD value of blank well) × 100%. The OD value was detected using a full-wavelength micrometer (Syngene H1; Syngene International, Bangalore, India). The best intervention conditions of the Chaiqi drug-containing serum should satisfy two requirements: 1, The OD value should be significant differently from the OD value of the blank serum at the same concentration and intervention time; 2, The cell activity rate should be the closest to 100%, but no more than 100%.

Western blotting analysis

Western blotting was performed as described previously [36]. Cell lysates and aortic homogenates were prepared in Radioimmunoprecipitation assay (RIPA) buffer (150 mM NaCl, 1% Triton X-100, 1% sodium deoxycholate, 50 mM Tris-HCl pH 7.5, 2 mM EDTA, 1 mM Pmetabolic syndromeF, 1 mM DTT, 1 mM Na_3VO_4, and 5 mM NaF) containing a protease inhibitor cocktail (Applygen Technologies Inc., Beijing, China) and a phosphatase inhibitor cocktail (Applygen Technologies Inc.). Proteins were separated by SDS-PAGE and transferred to polyvinylidene fluoride (PVDF) membranes. After blocking with 5% skim milk or 5% BSA, the membranes were incubated overnight at 4°C with primary antibodies recognizing beta-actin (1:1000), LC3B (1:1000), P62 (1:5000), phospho-eNOS (1:1000), eNOS (1:1000), ET-1 (1:5000), and Beclin 1 (1:2000). After incubation with the

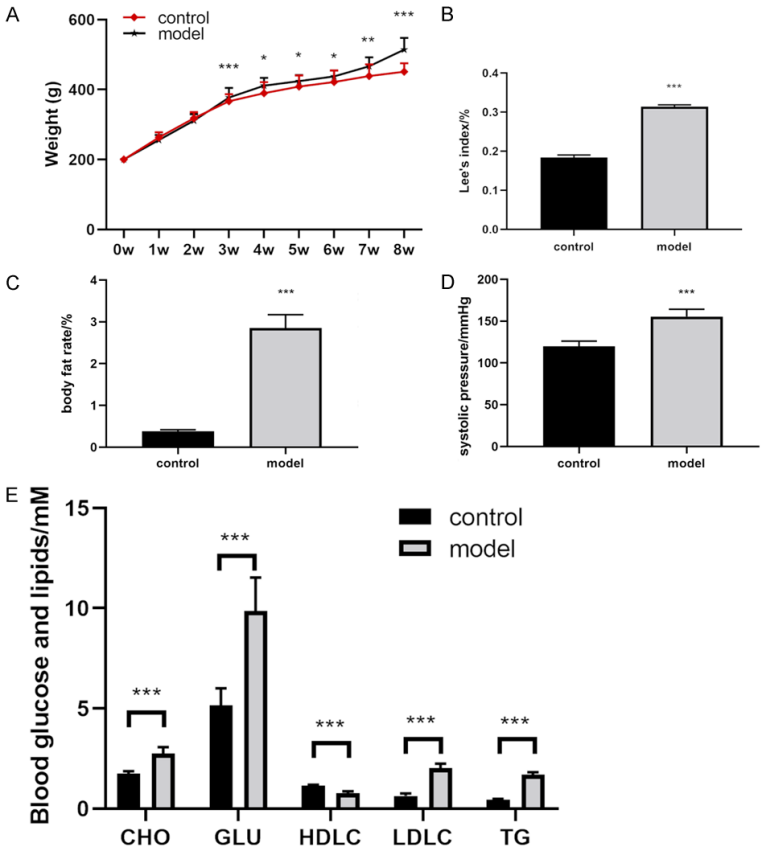

Figure 1. Effects of receiving the HSSFD for 8 weeks on SD rats. The comparison of (A) weight, (B) Lee's index, (C) body fat rate, (D) SBP determined using the non-invasive tail-cuff plethysmography method and recorded with an automatic sphygmotonography, (E) Glu and lipid levels measured using an automatic biochemical analyzer between the control and model group. Data are expressed as the mean ± SEM. *P < 0.05, **P < 0.01 and ***P < 0.001 versus the control; n = 7 per group.

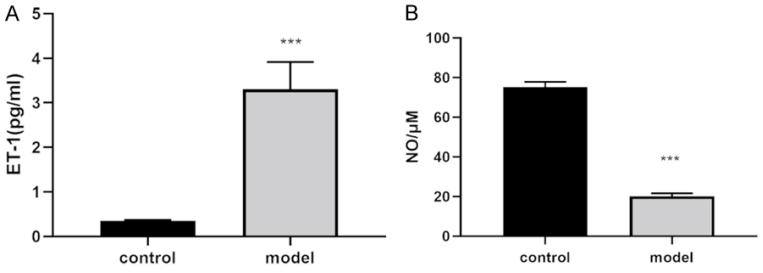

Figure 2. Effects of receiving the HSSFD for 8 weeks on SD rats. The comparison of serum (A) ET-1 and (B) NO expression measured using ELISA kits between the control and model groups. Data are expressed as the mean ± SEM. *P < 0.05, **P < 0.01, and ***P < 0.001 versus the Control; n = 7 per group.

HRP-conjugated secondary antibody (1:20000), the immunoreactive proteins were visualized using an enhanced chemiluminescence kit (ECL kit, Applygen Technologies Inc., Beijing, China) and an Immobilon Western Detection Reagents (Syngene G:BOX Chemi XX9, UK). Gray-scale levels of the immunoreactive protein bands were quantified using Image J (Media Cybernetics Inc.).

Statistical analysis

All the experiments repeated at least three times. The results are expressed as the mean ± SEM. The Komogorov-Smirnov test (sample size ≥ 5) and q-q map (sample size < 5) were used to analyze whether the normal distribution was satisfied. The rank-sum test was used for inter-group comparisons that did not meet the normal distribution, and Levene's test was used to determine the homogeneity of variance. The independent sample t test was used for inter-group comparisons when the variance was homogeneous, and the t' test was used when the variance was not homogeneous. SPSS 21.0 statistical software (IBM Corp., Armonk, NY, USA) was used for the statistical analysis. P < 0.05 was considered as statistically significant.

Results

HSSFD successfully induced metabolic syndrome related vascular endothelium injury in rats

As shown in **Figure 1**, the rats receiving HSSFD for 8 weeks showed markedly increased weight, Lee's index, body fat rate, SBP, glucose (Glu), cholesterol (CHO), triglycerides (TG), low density lipoprotein cholesterol (LDLC), and decreased high density lipoprotein cholesterol (HDLC) compared with the control rats. Moreover, as expected, serum ET-1 levels in the model rats were markedly increased compared with those in the control rats, while serum NO levels

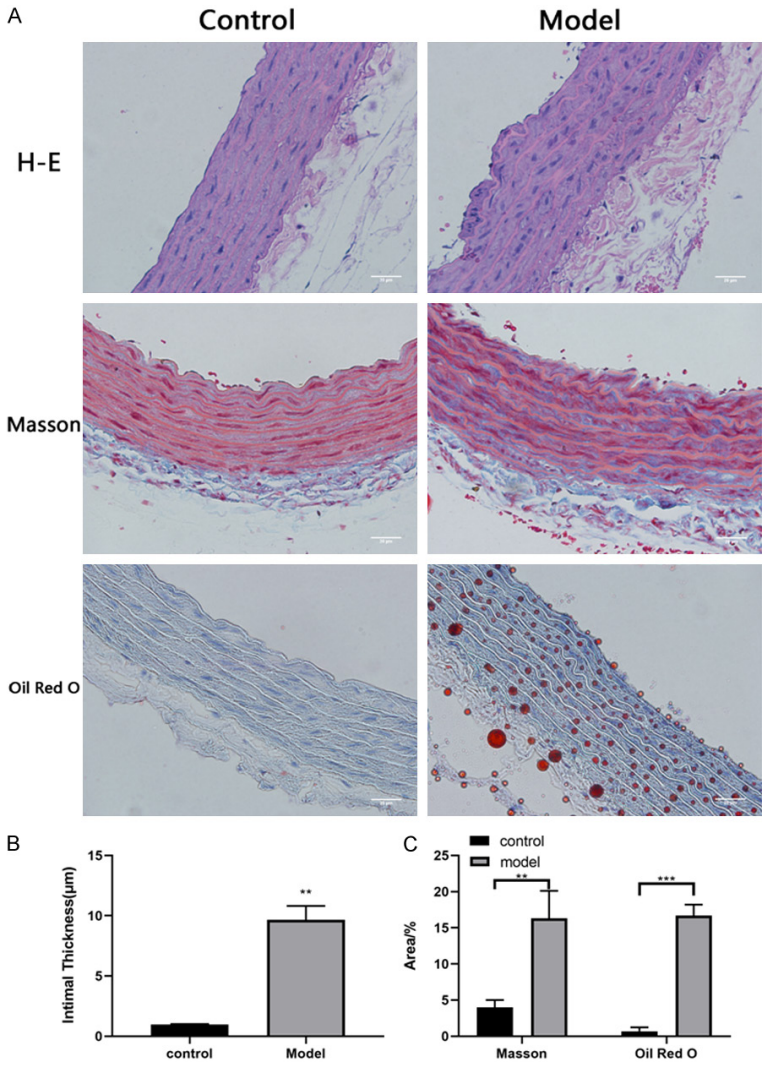

Figure 3. Histological analysis of the 400 × magnification thoracic aorta in the control and model groups. (A) In the model group we observed disorganized endothelial cells, thickened intima, and a variety of collagen and lipid droplets deposition by HE staining, Masson staining, and Oil Red O staining, compared with those of control group. We also observed greater (B) intimal thickness, (C) the deposition area of collagen and lipid droplet in the model group analyzed by Image J. The blue area presented by Masson staining is collagen deposition, and the red drops presented by Oil Red O staining are lipid droplet depositions. Bar: 20 μm, Data are expressed as the mean ± SEM. *P < 0.05, **P < 0.01, and ***P < 0.001 versus the control; n = 3 per group.

were greatly reduced (both P < 0.05. **Figure 2**). Images of HE staining, Masson staining, and Oil Red O staining revealed that the control thoracic aorta tissue had neatly arranged endothelial cells without thickened intima, or massive collagen and lipid droplet deposition (**Figure 3A**). In contrast, the model rats thoracic aorta tissue displayed disorganized endothelial cells, thickened intima, and varied levels of collagen and lipid droplets deposition (All P < 0.05. **Figure 3B**, **3C**). Our previous researches showed that serum VCAM-1, ICAM-1, IL-6, and TNF-a levels in the model rats were markedly increased compared with those in the control rats [27-29]. Taken together, the results demonstrated that administration of the HSSFD for 8 weeks can induce a rat model of vascular endothelial injury in metabolic syndrome.

Chaiqi decoction meliorates metabolic syndrome related vascular endothelial injury in vivo

After another 8 weeks of intervention, compared with the those of the model group, the weight, Lee's index, body fat rate, SBP, Glu, CHO, TG, and LDLC were decreased and HDLC was increased in the ND, ND+Rapa, and ND+Chaiqi groups. In terms of weight, Lee's index and SBP, the ND+Rapa and ND+Chaiqi groups performed better than the ND group. For TG, the ND+Chaiqi group performed better than both the ND and ND+Rapa groups (all P < 0.05. **Table 1**; **Figure 4**). Moreover, as the images of HE staining, Masson staining and Oil Red O staining (**Figure 5A**) showed, compared with the model group, the thickening of the intima and the area of collagen and lipid deposition in thoracic aorta tissue were significant ameliorated in the ND+Rapa and ND+Chaiqi groups, and to a greater extent in the ND+Chaiqi group than in the ND+Rapa group (All P < 0.05). However, there were no significant differences between the model group and ND group for intima thickness (P > 0.05. **Figure 5B**, **5C**). Furthermore, the ET-1 level in serum was decreased in the ND, ND+Rapa, and ND+Chaiqi groups compared with that in the model group,

Table 1. Effects of diet control, rapamycin, and Chaiqi decoction for 8 weeks on weight in rat models

group	Weight (g)								
	0 w	1 w	2 w	3 w	4 w	5 w	6 w	7 w	8 w
Control	462.71 ± 27.73	464.86 ± 27.99	475.00 ± 27.06	483.43 ± 24.49	487.00 ± 29.95	500.86 ± 29.17	504.86 ± 29.53	505.43 ± 30.60	510.71 ± 24.03
Model	509.29 ± 37.46*	514.14 ± 38.74*	521.14 ± 36.36*	524.86 ± 23.12**	534.43 ± 27.04**	548.71 ± 27.96**	565.43 ± 22.47**	568.57 ± 22.92**	585.14 ± 22.89***
ND	509.57 ± 36.65*	500.43 ± 35.18	490.29 ± 16.71$^{\&}$	508.86 ± 19.91	502.71 ± 20.42$^{\&}$	513.86 ± 24.89$^{\&}$	517.57 ± 18.65$^{\&\&}$	519.43 ± 21.33$^{\&\&}$	519.43 ± 18.08$^{\&\&\&}$
ND+Rapa	512.71 ± 37.89*	501.14 ± 33.14*	492.29 ± 23.73	493.00 ± 22.35$^{\&}$	478.14 ± 14.69$^{\&\&\&}$	490.86 ± 16.2$^{\&\&\&}$	500.00 ± 11.73$^{\&\&\&}$	495.14 ± 10.11$^{\&\&\&}$	499.71 ± 12.26$^{\&\&\&}$
ND+Chaiqi	511.71 ± 36.00*	509.00 ± 35.08*	477.29 ± 23.58$^{\&}$	482.29 ± 24.37$^{\&\&}$	472.29 ± 23.78$^{\&\&}$	486.00 ± 24.59$^{\&\&}$	487.86 ± 23.74$^{\&\&\&}$	478.00 ± 24.36$^{\&\&\&}$	481.86 ± 26.65$^{\&\&\&}$

n = 7, *P < 0.05, **P < 0.01, ***P < 0.001 *vs.* Control; $^{\&}$P < 0.05, $^{\&\&}$P < 0.01, $^{\&\&\&}$P < 0.001 *vs.* Model.

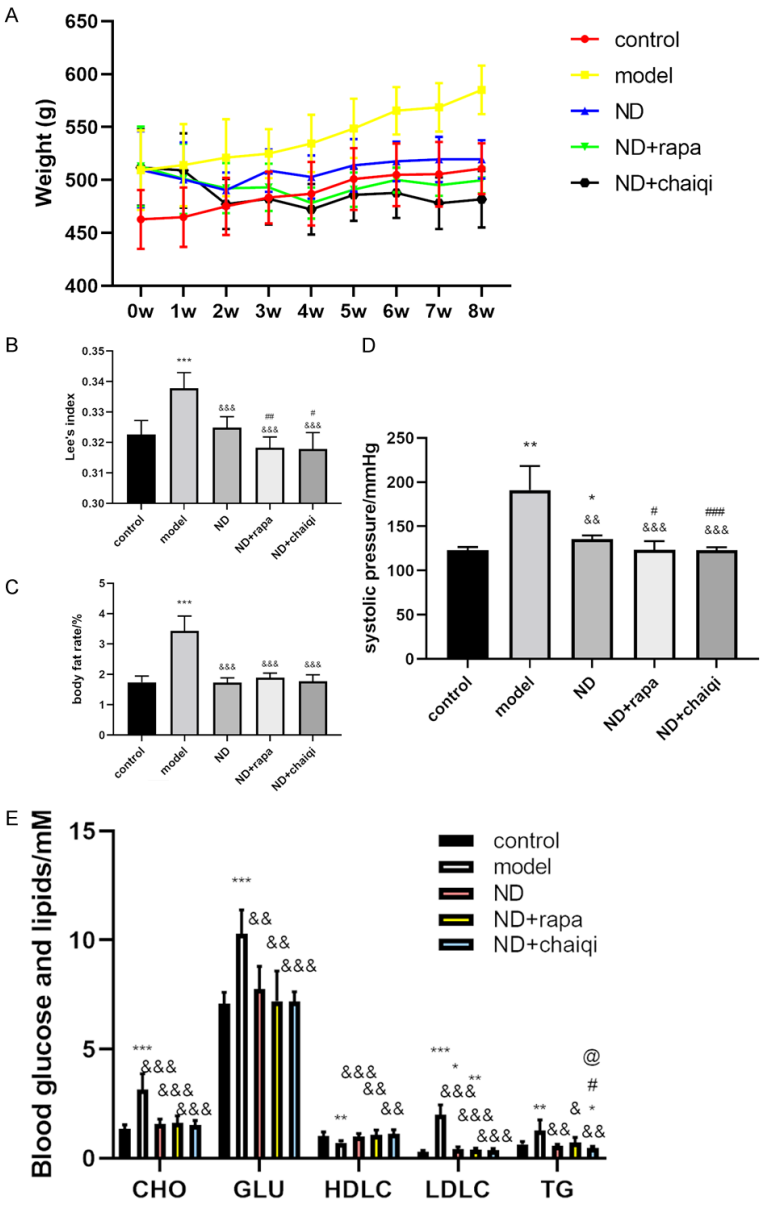

Figure 4. Effects of diet control, rapamycin, and Chaiqi decoction for 8 weeks on metabolic syndrome rats. (A) weight, (B) Lee's index, (C) body fat rate, (D) SBP was determined using the non-invasive tail-cuff plethysmography method and recorded using automatic sphygmotonography, (E) Glu and lipid level measured using an automatic biochemical analyzer. Data are expressed as mean ± SEM. *P < 0.05, **P < 0.01, and ***P < 0.001 versus the control; &P < 0.05, &&P < 0.01, and &&&P < 0.001 versus the Model; #P < 0.05, ##P < 0.01, and ###P < 0.001 versus ND; @P < 0.05, @@P < 0.01, and @@@P < 0.001 versus ND+Rapa; n = 7 per group.

while the ET-1 level was lower in the ND+Rapa and ND+Chaiqi groups than in the ND group (All P < 0.05. **Figure 6B**). The trend of ET-1 levels in thoracic aorta tissues were similar to that in serum, while the ET-1 level in the ND+Chaiqi samples was lower than that in the ND+Rapa samples (P < 0.05. **Figure 6A**). For NO, compared with that in the model group, the NO level in serum was increased in the ND, ND+Rapa, and ND+Chaiqi groups, with higher levels in the ND+Chaiqi group compared with those in the ND and ND+Rapa groups (All P < 0.05. **Figure 6D**). The trend of phosphorylation of eNOS in thoracic aorta tissues were similar to those in serum, while there were no significant differences between the ND+Chaiqi and ND+Rapa groups (P > 0.05. **Figure 6C**). Taken together, these results showed that the Chaiqi decoction meliorated metabolic syndrome-related vascular endothelial injury *in vivo* and the effect was better than that achieved by rapamycin and diet control only.

Chaiqi decoction ameliorates metabolic syndrome related vascular endothelial injury via autophagy activation

Rapamycin can suppress the mTOR signaling pathway and is an inducer of autophagy [37]. Therefore, we examined levels of autophagy-related factors (LC3, Beclin-1, p62), and the levels of autophagosomes and autolysosomes in rat thoracic aorta. As shown by the TEM images (**Figure 7A**), autophagosomes and autolysosomes could be recognized in the ND+Rapa and ND+Chaiqi groups. Furthermore, the IF images (**Figure 7B**) showed that compared with the control group, the integrated optical density of LC3 was decreased in the model and ND groups, while it was increased in the ND+Rapa and ND+Chaiqi groups (All P < 0.05. **Figure 7C**). Data from western blotting further confirmed the above-mentioned changes in autophagy levels.

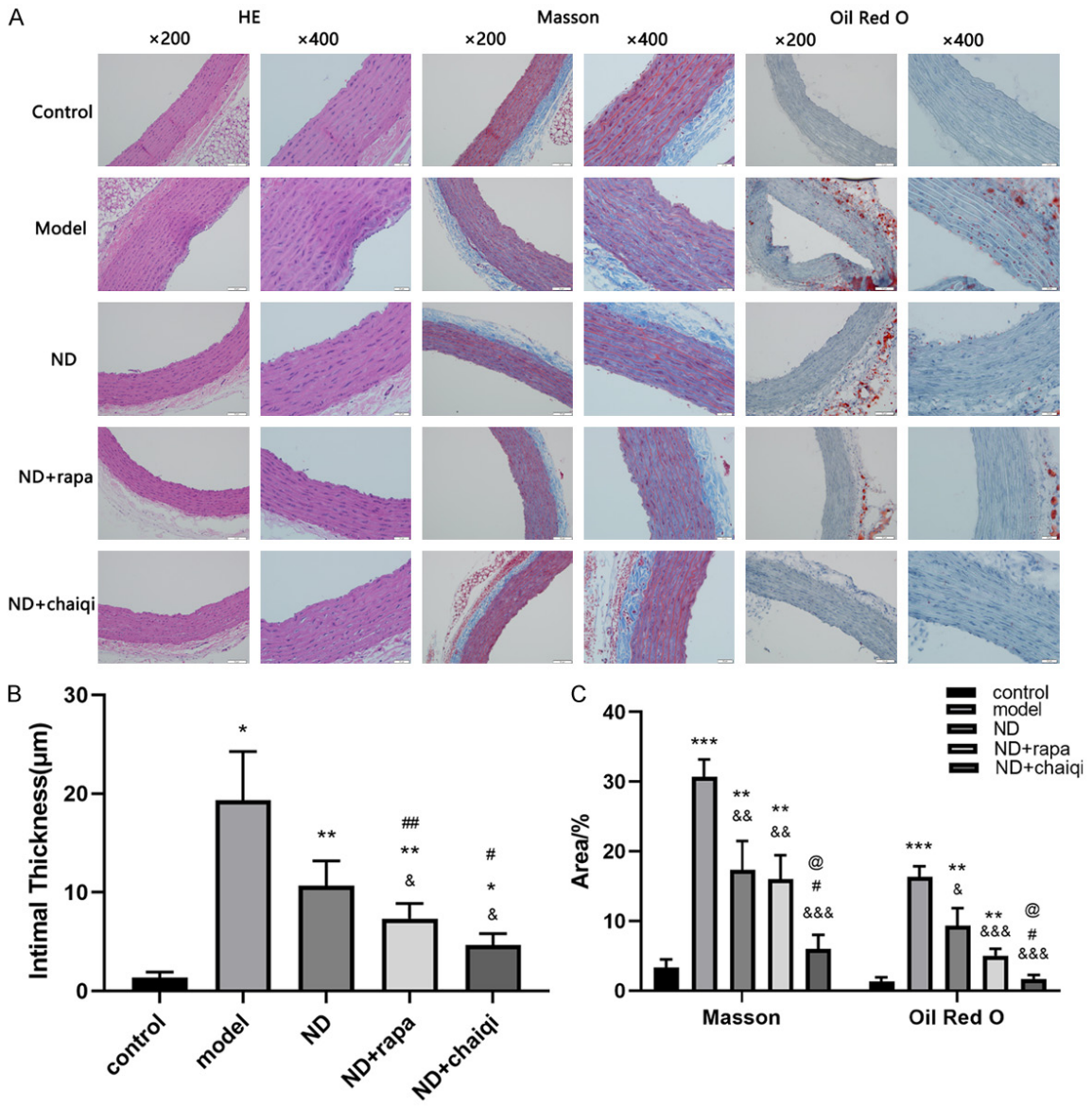

Figure 5. Histological analysis of the 200 ×/400 × magnification thoracic aorta in the experimental groups. (A) Representative images of HE staining, Masson staining, and Oil Red O staining of the rat thoracic aorta. Effects of receiving diet control, rapamycin, and Chaiqi decoction on intimal thickness (B) and the deposition of collagen and lipid droplets (C), analyzed using Image J. The blue area presented by Masson staining is collagen deposition, and the red drops presented by Oil Red O staining are lipid droplet deposition. Bar: 20 μm, Data are expressed as the mean ± SEM. Bar: 50 μm or 20 μm; *P < 0.05, **P < 0.01, and ***P < 0.001 versus the control; &P < 0.05, &&P < 0.01, and &&&P < 0.001 versus the model; #P < 0.05, ##P < 0.01, and ###P < 0.001 versus the ND; @P < 0.05, @@P < 0.01, and @@@P < 0.001 versus ND+Rapa; n = 3 per group.

Compared with the control group, the LC3II/I ratio (a useful marker for autophagy), and Beclin-1 levels were significantly decreased in the model and ND groups, while they were increased in the ND+Rapa and ND+Chaiqi groups (All P < 0.05. **Figure 8A**, **8B**). p62 (an autophagy adaptor protein) showed the reverse pattern (P < 0.05. **Figure 8C**). There was no significant difference between the ND+Rapa group and ND+Chaiqi group for LC3II/I, Beclin-1, and p62 (All P > 0.05).

Chaiqi drug-containing serum ameliorates metabolic syndrome-related vascular endothelial injury in vitro

Among the different intervention conditions whose OD value reached statistical significance

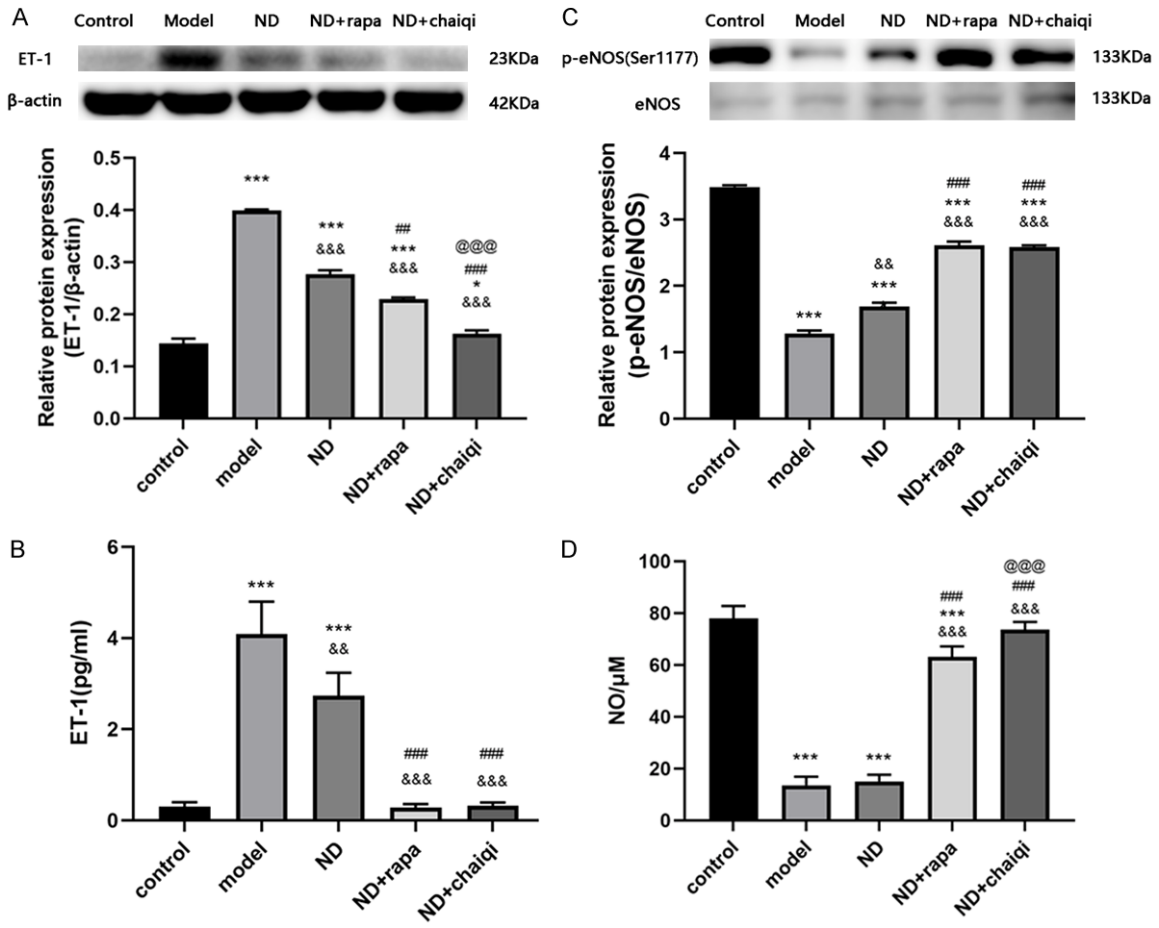

Figure 6. The expression of ET-1 and NO in thoracic aorta tissue and serum among the different experimental groups. Representative images and quantitative analysis of (A) ET-1 expression and (C) phosphorylation of eNOS in thoracic aorta tissue assessed using western blotting and Image J, respectively (n = 3 per group). The expression of (B) ET-1 and (D) NO in serum assessed using ELISA (n = 7 per group). Data are expressed as the mean ± SEM. *P < 0.05, **P < 0.01, and ***P < 0.001 versus the control; &P < 0.05, &&P < 0.01, and &&&P < 0.001 versus the model; #P <0.05, ##P < 0.01, and ###P < 0.001 versus ND; @P < 0.05, @@P < 0.01, and @@@P < 0.001 versus ND+Rapa.

compared with each blank group (**Table 2**), conditions comprising the Chaiqi drug-containing serum administered intragastrically for 7 days, intervention for 24 h, and a concentration of 10% could ameliorate the PA and hyperglycemia-induced reduction in cell viability by 99.41%. These condition was used for subsequent experiments, because its effect was the closest to 100%, without exceeding 100% (**Figure 9A**). Moreover, we evaluated the effect of Chaiqi drug-containing serum on ameliorating vascular endothelial injury by measuring ET-1 and NO levels. The ET-1 level in cells increased in the model and ND groups, and was not significantly different to that in ND+Rapa group, whereas the ET-1 level decreased in the ND+Chaiqi group compared with that in the control group (**Figure 9B**). The trend of ET-1 in cell culture supernatants was similar to that in cells, in which ND+Chaiqi group showed a higher ET-1 than that in the control group; however, the difference did not reach statistical significance (**Figure 9C**). The level of phosphorylated eNOS in cells decreased in the model group, but was not significantly different in the ND, ND+Rapa, and the ND+Chaiqi groups compared with that in the control group (**Figure 9D**), while the p-eNOS levels in the ND+Rapa and ND+chiqi groups were higher than that in the ND group. The NO levels in cell culture supernatants showed similar trends to the levels of p-eNOS in cells.

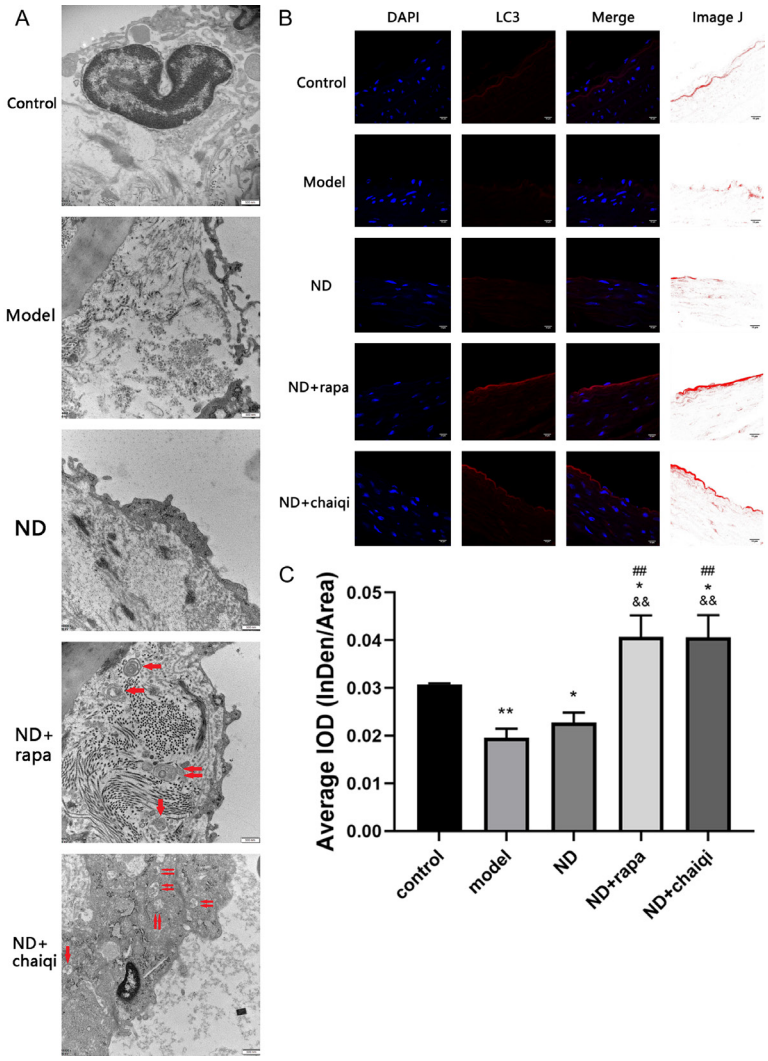

Figure 7. The number of autophagosomes and autolysosomes, and the expression of LC3 among different experimental groups. (A) Representative images of transmission electron microscopy of the rat thoracic aorta. The single arrows represent autophagosome and the double arrows represent autolysosomes. Bar = 500 nm. Representative image (B) and quantitative analysis (C) of LC3 expression in thoracic aorta tissue using immunofluorescence and Image J analysis, respectively. The blue spots represent cell nuclei and red puncta represent LC3. LC3 puncta were detected using anti-LC3 antibodies under a confocal laser scanning microscope. Bar = 10 μm; Data are expressed as the mean ± SEM. *P < 0.05, **P < 0.01, and ***P < 0.001 versus the control; &P < 0.05, &&P < 0.01, and &&&P < 0.001 versus the model; #P < 0.05, ##P < 0.01, and ###P < 0.001 versus ND; @P < 0.05, @@P < 0.01 and @@@P < 0.001 versus ND+Rapa; n = 3 per group.

There was no significant difference between the ND and model groups, and the ND+Chaiqi group had higher p-eNOS levels than the ND+Rapa group (**Figure 9E**). Taken together, these results supported the view that Chaiqi drug-containing serum ameliorates metabolic syndrome-related vascular endothelial injury *in vitro*, to a greater extent than rapamycin and nutrient control only.

Chaiqi drug-containing serum ameliorates vascular endothelial injury in vitro via autophagy activation

As shown by the TEM images (**Figure 10A**), autophagosomes and autolysosomes could be observed in the ND+Rapa and ND+Chaiqi groups. In addition, western blotting revealed that, the LC3II/I ratio were significantly decreased in the model and ND groups, but increased in the ND+Rapa and ND+Chaiqi groups (All P < 0.05. **Figure 11A**). The trend of Beclin-1 was similar to the LC3II/I ratio, while its level in the ND group was higher than that in the model group (All P < 0.05. **Figure 11B**). However, p62 showed the reverse pattern (All P < 0.05. **Figure 11C**). Furthermore, we transfected a GFP-mRFP-LC3-expressing adenovirus into cultured HUVECs because it is difficult to assess autophagy flux *in vivo*, especially in vascular tissue. Images (**Figure 10B**) and related data (**Figure 10C**) in the transfected HUVECs further confirmed the abovementioned changes in autophagy levels. Compared with the control group, both autolysosomes (red dots) and autophagosomes (yellow dots) were significantly decreased in the model group, and increased in the ND+Rapa and ND+Chaiqi groups. There were no significant differences between the control and ND groups. In addition, there was no statistical significance between the ND+Rapa and ND+Chaiqi groups.

Chaiqi drug-containing serum upregulated autophagy in a time-dependent manner

To assess autophagy flux of Chaiqi drug-containing serum dynamically, cells after intervention were preincubated with DALGreen and

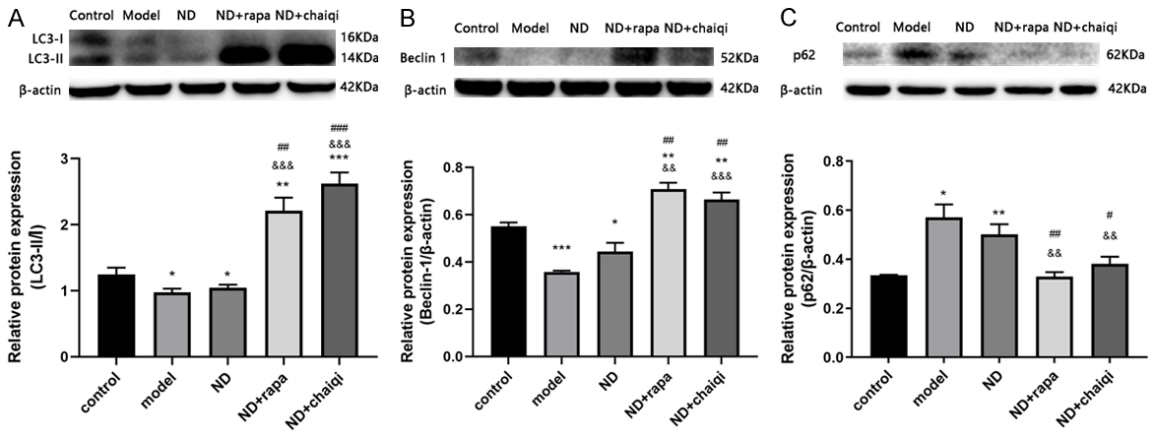

Figure 8. The expression of autophagy-related proteins in thoracic aorta tissue among the different experimental groups. Representative image and quantitative analysis of the expression of (A) LC3B, (B) Beclin-1, and (C) p62 by western blotting and Image J, respectively. Data are expressed as the mean ± SEM. *P < 0.05, **P < 0.01, and ***P < 0.001 versus the control; &P < 0.05, &&P < 0.01, and &&&P < 0.001 versus the model; #P < 0.05, ##P < 0.01, and ###P < 0.001 versus ND; @P < 0.05, @@P < 0.01, and @@@P < 0.001 versus ND+Rapa. n = 3 per group.

Table 2. OD values of different conditions of Chaiqi drug-containing serum intervention in HUVECs injured by PA and hyperglycemia

group		OD				
		5%	10%	15%	20%	30%
24 h	B	0.75 ± 0.01	0.89 ± 0.02	0.90 ± 0.03	0.87 ± 0.08	0.84 ± 0.04
	d3	0.76 ± 0.01	0.89 ± 0.02	0.86 ± 0.02*	0.83 ± 0.03	0.82 ± 0.02
	d5	0.90 ± 0.06***	1.28 ± 0.11***	0.99 ± 0.15	0.89 ± 0.09	0.90 ± 0.14
	d7	0.89 ± 0.05***	1.02 ± 0.11**	0.89 ± 0.09	0.82 ± 0.06	0.92 ± 0.11
48 h	B	0.89 ± 0.07	1.22 ± 0.03	1.22 ± 0.02	1.34 ± 0.04	1.22 ± 0.04
	d3	0.85 ± 0.03	1.29 ± 0.03***	1.47 ± 0.11***	1.38 ± 0.05	1.38 ± 0.12**
	d5	1.08 ± 0.05***	1.54 ± 0.20***	1.64 ± 0.14***	1.47 ± 0.20	1.47 ± 0.18**
	d7	1.24 ± 0.16***	1.54 ± 0.20***	1.49 ± 0.16***	1.51 ± 0.18*	1.31 ± 0.13
72 h	B	0.96 ± 0.02	1.26 ± 0.14	1.43 ± 0.11	1.64 ± 0.04	1.54 ± 0.04
	d3	0.87 ± 0.01***	1.26 ± 0.14	1.41 ± 0.14	1.76 ± 0.16*	1.56 ± 0.03
	d5	1.25 ± 0.13***	1.74 ± 0.12***	1.80 ± 0.07***	1.61 ± 0.12	1.69 ± 0.03***
	d7	1.65 ± 0.12***	1.71 ± 0.08***	1.73 ± 0.12***	1.68 ± 0.07***	1.60 ± 0.11

B: Blank serum group; d3, d5, and d7: Chaiqi drug-containing serum administered intragastrically for 3 days, 5 days, and 7 days, respectively. *P < 0.05, **P < 0.01, ***P < 0.001 *vs*. the blank serum group.

DAPRed to stain autolysosomes and autophagosomes. As shown in **Figure 12A**, compared with 0 h, both the green and red fluorescent areas increased significantly at 12 h, 18 h, and 24 h, and the stained areas increased with time (**Figure 12B**). The LC3II/I ratio also increase with time (**Figure 12C**). This indicated that Chaiqi drug-containing serum upregulated autophagy in a time-dependent manner.

Discussion

The vascular endothelium is an important cellular component of the cardiovascular system and plays a crucial role in maintaining cardiovascular homeostasis. Therefore, endothelial dysfunction is the one of the earliest detectable vascular abnormalities and is predictive of later cardiovascular complications [38-40]. Animal experiments have provided ample evidence that metabolic syndrome is strongly associated with vascular endothelial injury. Feeding with an HSSFD induced abnormalities of metabolic syndrome-related indices, such as abdominal fat deposition, abnormal glucose tolerance, dyslipidemia, hyperinsulinemia, and hypertension. It also led to vascular endothelial

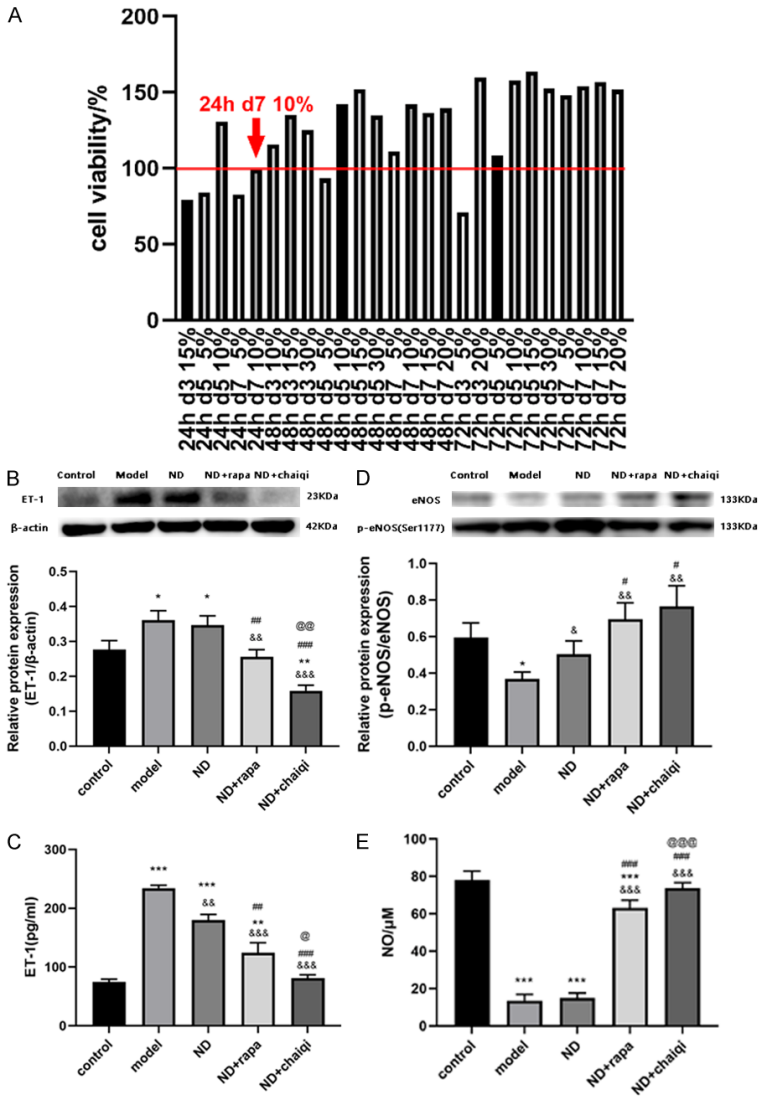

Figure 9. Screening of Chaiqi drug-containing serum and the levels of ET-1 and NO among the different experimental groups. (A) CCK-8 screening showing that he best intervention conditions comprised intragastric administration for 7 days, intervention for 24 h, and a concentration of 10%. Representative images and quantitative analysis of (B) ET-1 levels and (D) the phosphorylation of eNOS in cells using western blotting and Image J, respectively. The levels of (C) ET-1 and (E) NO in cell culture supernatants, as assessed using ELISA. Data are expressed as the mean ± SEM. *P < 0.05, **P < 0.01, and ***P < 0.001 versus the control; &P < 0.05, &&P < 0.01, and &&&P < 0.001 versus the model; #P < 0.05, ##P < 0.01, and ###P < 0.001 versus ND; @P < 0.05, @@P < 0.01, and @@@P < 0.001 versus ND+Rapa.

dysfunction via an inflammatory reaction and oxidative stress, accompanied by increased ET-1 and decreased of NO levels [41-46]. Besides, a clinical study indicated that free fatty acid levels in patients with diabetes were 50% higher compared with those in healthy controls during overnight fasting, and postprandial levels of palmitate (one of the predominant saturated fatty acids) were nearly three times higher than in the healthy controls [47]. Palmitate also inhibited cell proliferation and induced apoptosis in mice aortic endothelial cells, which were separated from mice fed high-calorie and high-cholesterol diets for 3 months [48]. The lipotoxic effect of PA has been implicated in the pathogenesis of numerous CVDs [49]. In our study, to mimic the vascular endothelial dysfunction caused by HSSFD and the constant exposure of vascular endothelial cells to the condition of chronic hyperglycemia and PA, we utilized a rat model fed with HSSFD containing 5% PA and a cell model maintained and passaged in media containing 25 mM glucose that were further acutely challenged with 0.4 mM PA according to a previously published protocol [25, 27-29], to gain a better understanding of the pathological effects of vascular endothelial injury in metabolic syndrome. Moreover, previous studies lack an evaluation of diet or nutrient controls. To explore the effect of diet control in improving vascular endothelial injury in metabolic syndrome, this study conducted intervention on the basis of diet and nutrient control.

The mammalian target of rapamycin (mTOR) is an evolutionarily conserved serine/threonine kinase that senses fluctuations in extracellular and intracellular nutrients to modulate cellular growth, metabolism, and survival [50, 51]. Additionally, the mTOR inhibitor rapamycin (Rapa, also known as sirolimus) has vital uses in CVDs [52, 53], oncology [54], and transplantation medicine [55], especially in metabolic disorders such as diabetic nephropathy [56, 57], diabetic retinop-

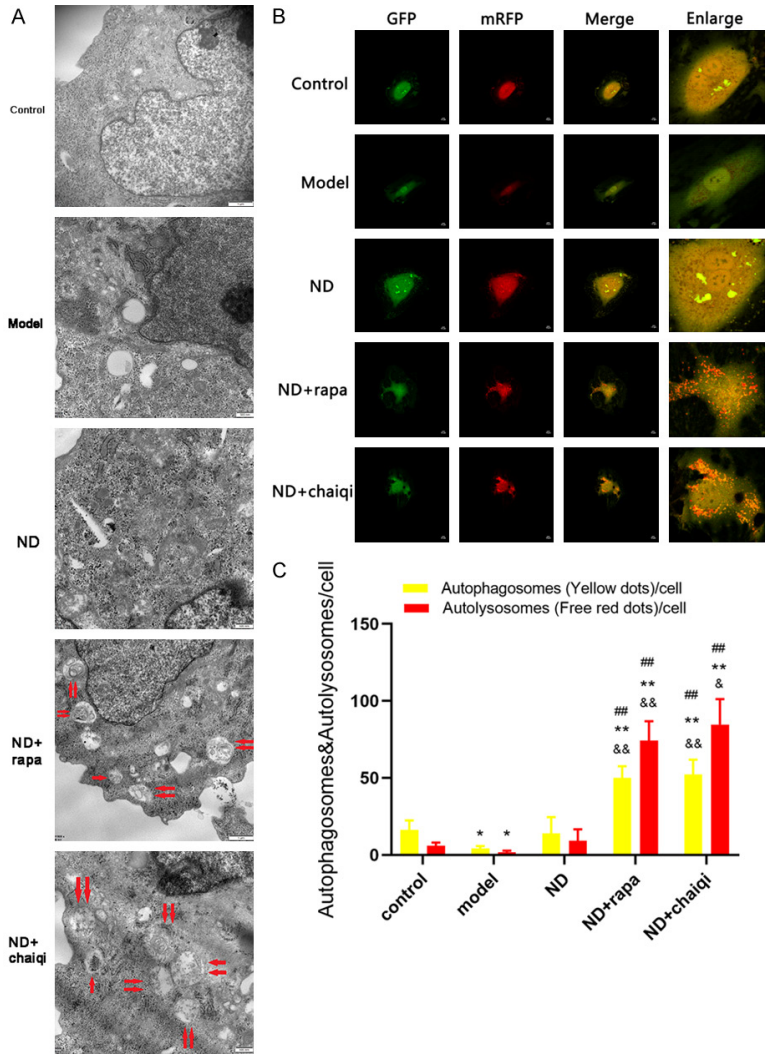

Figure 10. The number of autophagosomes and autolysosomes among the different experimental groups. (A) Representative images of transmission electron microscopy in cells. The single arrows represent autophagosomes and the double arrows represent autolysosomes. Bar = 1 μm or 500 nm. To assess autophagy flux of different interventions, a GFP-mRFP-LC3 adenovirus was transfected into cultured HUVECs for 5 h at an MOI of 100. (B) Representative images and (C) quantitative analysis of autophagosome and autolysosome numbers by manual counting. The yellow puncta represent autophagosomes and red puncta represent autolysosomes, which were detected under confocal laser scanning microscope. Bar = 10 μm; Data are expressed as the mean ± SEM. *P < 0.05, **P < 0.01, and ***P < 0.001 versus the control; &P < 0.05, &&P < 0.01, and &&&P < 0.001 versus the model; #P < 0.05, ##P < 0.01, and ###P < 0.001 versus ND; @P < 0.05, @@P < 0.01, and @@@P < 0.001 versus ND+Rapa; n = 3 per group.

athy [58], diabetic heart disease [59], and metabolic syndrome [60] by targeting mTOR. Studies have shown that mTOR activity in mice with type 2 diabetes is significantly increased [61], and rapamycin can reduce body weight and fat mass, and improve insulin resistance and blood glucose levels by inhibiting mTOR activity [32, 62]. Besides, it can also decrease ET-1 levels and the aggregation of platelets and neutrophils, reduce the release of cellular chemokines and the migration of vascular smooth muscle cells to the intimal layer, and improve intimal hyperplasia [52]. Moreover, rapamycin exhibits protective effects on endothelial cells in metabolic syndrome by inducing autophagy, reducing apoptosis and endoplasmic reticulum stress [63], improving the activity of NO and phosphorylation of eNOS, and decreasing ET-1 levels [53, 64]. In addition, rapamycin significantly inhibited glucose and palmitate treatment-induced apoptosis and inflammation, which indicated that the induction of autophagy by rapamycin might have a beneficial effect on diabetic atherosclerosis [25]. In the present study, we found that diet and nutrient control and intervention with rapamycin or the Chaiqi decoction improved the abnormalities in metabolic syndrome-related indices (weight, lee's index, body fat rate, SBP, Glu, CHO, TG, HDLC, and LDLC) and vascular endothelial injury-related indices (intimal thickness, collagen, and lipid droplet deposition, ET-1, NO, and phosphorylation of eNOS) *in vivo* and *in vitro*. Notably, Chaiqi was more effective in reducing the deposition of collagen and lipid droplets, increasing NO in serum and cell culture supernatants, and decreasing ET-1 in cells, tissue, and cell culture supernatants than rapamycin. Diet and nutrient control was the least effective and showed no significant difference with the model group in terms of intimal thickness, cellular ET-1 levels, and NO levels in serum and cell culture supernatants. These results indicated that Chaiqi could not only improve the abnormalities in metabolic syn-

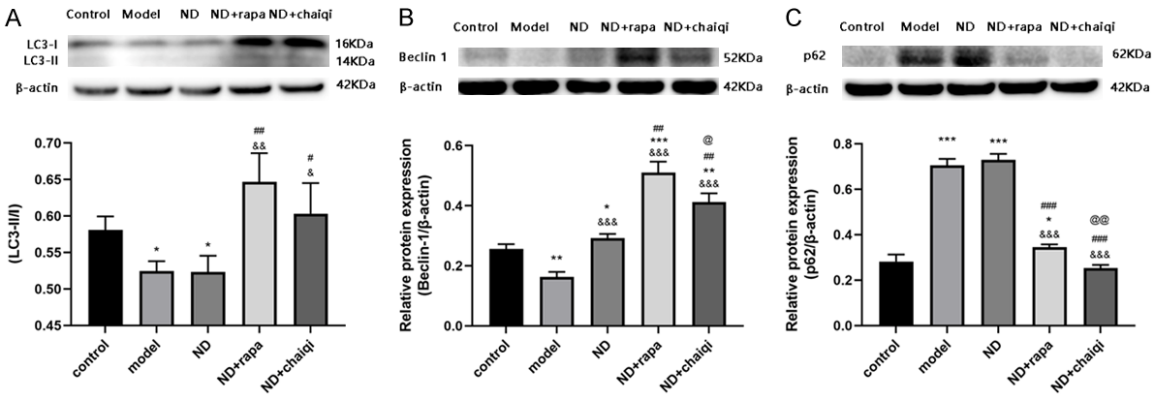

Figure 11. The levels of autophagy-related proteins in cells among the different experimental groups. Representative images and quantitative analysis of the levels of (A) LC3B, (B) Beclin-1, and (C) p62, assessed using western blotting and Image J, respectively. Data are expressed as the mean ± SEM. *P < 0.05, **P < 0.01, and ***P < 0.001 versus the control; &P < 0.05, &&P < 0.01, and &&&P < 0.001 versus the model; #P < 0.05, ##P < 0.01, and ###P < 0.001 versus ND; @P < 0.05, @@P < 0.01, and @@@P < 0.001 versus ND+Rapa.

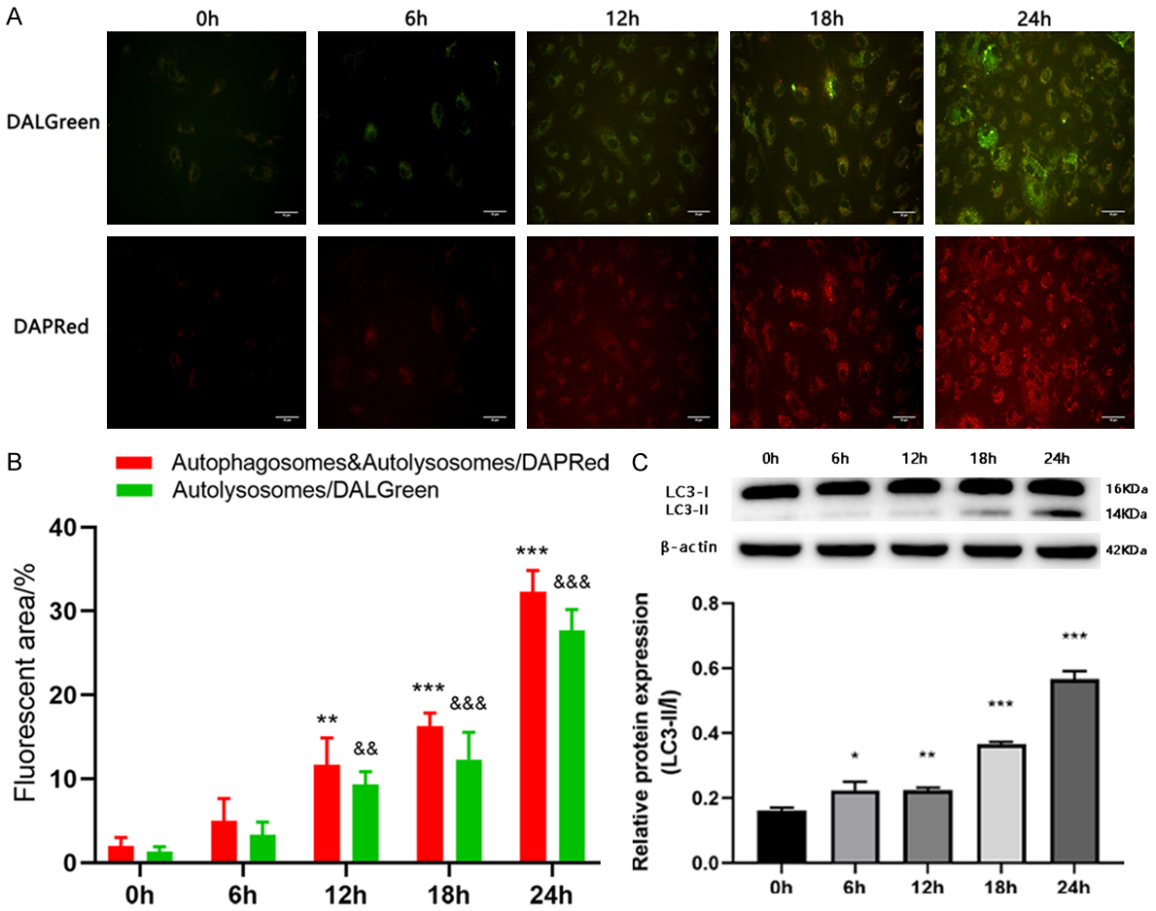

Figure 12. Effects of Chaiqi drug-containing serum on autophagy flux in HUVECs injured by PA and hyperglycemia. To assess autophagy flux of Chaiqi drug-containing serum dynamically, cells after intervention were incubated with DALGreen and DAPRed in the culture medium for 1 h at 37 °C. (A) Representative images were detected by immunofluorescence assay and (B) quantitative analysis of autophagosome and autolysosome expression was performed using Image J. Green (DALGreen) represents the autolysosomes and red (DAPRed) represents both autolysosomes and autophagosomes. Bar = 10 μm. Representative images and quantitative analysis of the expression of LC3B (C) in cells were assessed using western blotting. Data are expressed as the mean ± SEM. *P < 0.05, **P < 0.01 and ***P < 0.001 versus 0 h.

drome-related indices, but could also ameliorate vascular endothelial injury in metabolic syndrome.

Autophagy is a catabolic process in eukaryotic cells that relies on lysosomes to degrade old proteins and dysfunctional organelles, and participates in cell development, differentiation, and maintenance of homeostasis [65]. In recent years, autophagy has been shown to participate in the pathogenesis of various CVDs, such as cardiomyopathy [66], heart failure [67], atherosclerosis [68], and myocardial ischemia/reperfusion injury [69]. In metabolic syndrome, high glucose and fat status can increase the production of reactive oxygen species and the expression of cell surface adhesion molecules, induce inflammatory changes, leading to vascular endothelial injury, accompanied by autophagy inhibition, which act as a protective mechanism against apoptosis [7, 70, 71]. Cui et al. showed that metabolic syndrome in rats induced by a high fat diet and 10% fructose water feeding resulted in hypertension, obesity, metabolic abnormity, insulin resistance, downregulated p-eNOS levels, vascular endothelial injury, and autophagy dysfunction. All these abnormalities in metabolic syndrome rats were ameliorated after restoring autophagy [7]. In a separate study, treatment of endothelial cells with high concentrations of glucose and PA impaired basal autophagy, which resulted in increased cell apoptosis and inflammation [25]. Collectively, these results suggested that the induction of an autophagic response in endothelial cells exerts cytoprotective actions under excess nutrient-induced stress. However, some studies have shown that glucose and palmitate induce autophagy in endothelial cells [72-74]. These opposite effects might depend on concentration, intervention time, and different cell conditions. To date, various naturally occurring agents, such as Curcumin [74, 75], Resveratrol [76, 77], Berberine [78], Royal Jelly [79], and Naringenin [80], have been reported to have cardiovascular protective effects via upregulating autophagy in endothelial cells. Interestingly, these mentioned above agents are mostly ingredients of TCM. The effects of Chinese herbal compound prescription, including Chaiqi decoction, have not been examined. In the present study, we found that autophagy was impaired after metabolic syndrome-related vascular endothelial injury and diet/nutrient control might not effectively improve the level of autophagy *in vivo* and *in vitro*. However, Chaiqi could upregulate autophagy similarly to the autophagy inducer rapamycin. Notably, autophagy flux analysis indicated that there was no statistically significant difference between Chaiqi and rapamycin for the count of autophagosomes and autolysosomes and the levels of autophagy-related proteins. Furthermore, we assessed autophagy flux of Chaiqi drug-containing serum dynamically by incubating with DALGreen and DAPRed and found that Chaiqi drug-containing serum upregulated autophagy in a time-dependent manner. These results indicated that Chaiqi could ameliorate vascular endothelial injury in metabolic syndrome by upregulating autophagy.

There have been many studies on the regulation of hunger-induced autophagy, involving the regulation of activity of several kinases, including mammalian target of rapamycin Complex 1 (mTORC1), unc-51 like autophagy activating kinase 1 (ULK1), and Adenosine 5'-monophosphate (AMP) activated protein kinase (AMPK) [81, 82]. Under low nutrient conditions, these kinases (and other kinases) coordinate the formation of autophagosomes, which are digested by proteases in lysosomes and break down the products for subsequent synthesis of new proteins or to fuel cells [83]. However, the autophagy regulation mechanism of endothelial cells has not been fully determined under high-nutrient states (such as metabolic syndrome) [25]. Under excess nutrient conditions, AMPK activity and the phosphorylation of AMPK and ULK1 were diminished, accompanied by impaired basal autophagy [25, 84] in human aortic endothelial cells. Intriguingly, reactivation of AMPK with activators AICAR, A769662, or phenformin failed to restore autophagy, while the mTOR inhibitor rapamycin significantly induced autophagy [25]. mTOR is usually activated under high nutrient conditions, which would explain that the uncoupling of AMPK from ULK1 activation under high glucose and palmitate conditions occurs because AMPK can no longer access and interact with ULK1 because of mTOR activation. However, increased levels of phosphorylated (Thr389) p70S6K and the ratio of phosphorylated (Ser2448) mTOR to total mTOR protein were not observed [25]. It is possible that the failure to

detect increased mTOR activity might have been caused by the lack of a time-course study under these conditions, because high nutrient levels lead to mTOR activation [85]. In this regard, we found that autophagy was suppressed during vascular endothelial injury in metabolic syndrome. Chaiqi could restore metabolic syndrome-induced abnormalities similarly to the mTOR inhibitor rapamycin. Our further experiments will investigate whether Chaiqi decoction could upregulate autophagy via the mTOR signalling pathway.

Conclusions

In conclusions, our findings demonstrated that the Chaiqi decoction ameliorated vascular endothelial injury by enhancing autophagy. Our study provides additional insights into the clinical application of TCM in metabolic syndrome and related cardiovascular complications.

Acknowledgements

The study was supported by the self-selected topic of the Beijing University of Chinese Medicine (Grant no. 2019-JYB-JS-114).

Disclosure of conflict of interest

None.

Address correspondence to: Dr. Li-Ping Zhang, Beijing University of Chinese Medicine, No.11 Bei San Huan Dong Lu, Chaoyang District, Beijing 100029, China. E-mail: lpzhang2005@126.com; Dr. Jing Liu, Dongfang Hospital of Beijing University of Chinese Medicine, Fangxingyuan, Fangzhuang, Fengtai District, Beijing 100078, China. E-mail: liujing20120114@163.com

References

[1] Dommermuth R and Ewing K. Metabolic syndrome systems thinking in heart disease. Prim Care 2018; 45: 109-129.

[2] Mottillo S, Filion KB, Genest J, Joseph L, Pilote L, Poirier P, Rinfret S, Schiffrin EL and Eisenberg MJ. The metabolic syndrome and cardiovascular risk a systematic review and meta-analysis. J Am Coll Cardiol 2010; 56: 1113-1132.

[3] Berwick ZC, Dick GM and Tune JD. Heart of the matter: coronary dysfunction in metabolic syndrome. J Mol Cell Cardiol 2012; 52: 848-56.

[4] Rawshani A, Sattar N, Franzén S, Rawshani A, Hattersley AT, Svensson AM, Eliasson B and Gudbjörnsdottir S. Excess mortality and cardiovascular disease in young adults with type 1 diabetes in relation to age at onset: a nationwide, register-based cohort study. Lancet 2018; 392: 477-486.

[5] Sitia S, Tomasoni L, Atzeni F, Ambrosio G, Cordiano C, Catapano A, Tramontana S, Perticone F, Naccarato P, Camici P, Picano E, Cortigiani L, Bevilacqua M, Milazzo L, Cusi D, Barlassina C, Sarzi-Puttini P and Turiel M. From endothelial dysfunction to atherosclerosis. Autoimmun Rev 2010; 9: 830-834.

[6] Tziomalos K, Athyros VG, Karagiannis A and Mikhailidis DP. Endothelial dysfunction in metabolic syndrome: prevalence, pathogenesis and management. Nutr Metab Cardiovasc Dis 2010; 20: 140-146.

[7] Cui F, Guan Y, Guo J, Tian YM, Hu HF, Zhang XJ and Zhang Y. Chronic intermittent hypobaric hypoxia protects vascular endothelium by ameliorating autophagy in metabolic syndrome rats. Life Sci 2018; 205: 145-154.

[8] Samsamshariat SZA, Sakhaei F, Salehizadeh L, Keshvari M and Asgary S. Relationship between resistin, endothelin-1, and flow-mediated dilation in patient with and without metabolic syndrome. Adv Biomed Res 2019; 8: 16.

[9] Beghetti M, Black SM and Fineman JR. endothelin-1 in congenital heart disease. Pediatr Res 2005; 57: 16r-20r.

[10] da Silva AA, Kuo JJ, Tallam LS and Hall JE. Role of endothelin-1 in blood pressure regulation in a rat model of visceral obesity and hypertension. Hypertension 2004; 43: 383-387.

[11] Iglarz M, Steiner P, Wanner D, Rey M, Hess P and Clozel M. Vascular effects of endothelin receptor antagonists depends on their selectivity for ETA versus ETB receptors and on the functionality of endothelial ETB receptors. J Cardiovasc Pharmacol 2015; 66: 332-337.

[12] Mazzuca MQ and Khalil RA. Vascular endothelin receptor type B: structure, function and dysregulation in vascular disease. Biochem Pharmacol 2012; 84: 147-162.

[13] Rocha NG, Templeton DL, Greiner JJ, Stauffer BL and DeSouza CA. Metabolic syndrome and endothelin-1 mediated vasoconstrictor tone in overweight/obese adults. Metabolism 2014; 63: 951-956.

[14] Yu AP, Tam BT, Yau WY, Chan KS, Yu SS, Chung TL and Siu PM. Association of endothelin-1 and matrix metallopeptidase-9 with metabolic syndrome in middle-aged and older adults. Diabetol Metab Syndr 2015; 7: 111.

[15] Förstermann U and Münzel T. Endothelial nitric oxide synthase in vascular disease: from marvel to menace. Circulation 2006; 113: 1708-1714.

[16] Wyatt AW, Steinert JR and Mann GE. Modulation of the L-arginine/nitric oxide sig-

nalling pathway in vascular endothelial cells. Biochem Soc Symp 2004; 143-156.
[17] Sessa WC. eNOS at a glance. J Cell Sci 2004; 117: 2427-2429.
[18] Gao L, Siu KL, Chalupsky K, Nguyen A, Chen P, Weintraub NL, Galis Z and Cai H. Role of uncoupled endothelial nitric oxide synthase in abdominal aortic aneurysm formation: treatment with folic acid. Hypertension 2012; 59: 158-166.
[19] Choi AM, Ryter SW and Levine B. Autophagy in human health and disease. N Engl J Med 2013; 368: 651-662.
[20] Tan Y, Gong Y, Dong M, Pei Z and Ren J. Role of autophagy in inherited metabolic and endocrine myopathies. Biochim Biophys Acta Mol Basis Dis 2019; 1865: 48-55.
[21] Ren J, Sowers JR and Zhang Y. Metabolic stress, autophagy, and cardiovascular aging: from pathophysiology to therapeutics. Trends Endocrinol Metab 2018; 29: 699-711.
[22] Zhang Y, Whaley-Connell AT, Sowers JR and Ren J. Autophagy as an emerging target in cardiorenal metabolic disease: from pathophysiology to management. Pharmacol Ther 2018; 191: 1-22.
[23] Ren SY and Xu X. Role of autophagy in metabolic syndrome-associated heart disease. Biochim Biophys Acta 2015; 1852: 225-231.
[24] Kosacka J, Nowicki M, Paeschke S, Baum P, Blüher M and Klöting N. Up-regulated autophagy: as a protective factor in adipose tissue of WOKW rats with metabolic syndrome. Diabetol Metab Syndr 2018; 10: 13.
[25] Weikel KA, Cacicedo JM, Ruderman NB and Ido Y. Glucose and palmitate uncouple AMPK from autophagy in human aortic endothelial cells. Am J Physiol Cell Physiol 2015; 308: C249-263.
[26] Sun SY. Observation on the clinical effect of Chaiqi decoction on 78 cases of metabolic syndrome. Hebei Chinese Medicine 2014; 36: 1788-1789+1830.
[27] Wang Y, Liu J, Wang XX and Zhang LP. Effects of Chaiqi decoction on glucose and lipid metabolism and insulin resistance in rats with metabolic syndrome. Journal of Beijing University of Chinese Medicine 2015; 38: 597-600.
[28] Liu J, Zhang LP, Wang Y, Wang XX, Zheng H and Yan Y. Study on the mechanism of Chaiqi decoction interfering metabolic syndrome. Journal of Beijing University of Chinese Medicine 2012; 35: 673-678+721.
[29] Chen LR, Liu Y, Zhang JY, Peng P and Zhang LP. Study on the intervention mechanism of Chaiqi decoction in the prevention and treatment of vascular injury in rats with metabolic syndrome. Journal of Chinese Medicine Information 2017; 34: 39-44.
[30] Dan HC and Baldwin AS. Differential involvement of IkappaB kinases alpha and beta in cytokine- and insulin-induced mammalian target of rapamycin activation determined by Akt. J Immunol 2008; 180: 7582-7589.
[31] Zhou YD, Cao XQ, Liu ZH, Cao YJ, Liu CF, Zhang YL and Xie Y. Rapamycin inhibits oxidized low density lipoprotein uptake in human umbilical vein endothelial cells via mTOR/NF-κB/LOX-1 pathway. PLoS One 2016; 11: e0146777.
[32] Zhou W and Ye S. Rapamycin improves insulin resistance and hepatic steatosis in type 2 diabetes rats through activation of autophagy. Cell Biol Int 2018; 42: 1282-1291.
[33] Bernardis LL and Patterson BD. Correlation between 'Lee index' and carcass fat content in weanling and adult female rats with hypothalamic lesions. J Endocrinol 1968; 40: 527-528.
[34] Kimura S, Noda T and Yoshimori T. Dissection of the autophagosome maturation process by a novel reporter protein, tandem fluorescent-tagged LC3. Autophagy 2007; 3: 452-460.
[35] Iwashita H, Sakurai HT, Nagahora N, Ishiyama M, Shioji K, Sasamoto K, Okuma K, Shimizu S and Ueno Y. Small fluorescent molecules for monitoring autophagic flux. FEBS Lett 2018; 592: 559-567.
[36] Kee HJ, Kim JR, Nam KI, Park HY, Shin S, Kim JC, Shimono Y, Takahashi M, Jeong MH, Kim N, Kim KK and Kook H. Enhancer of polycomb1, a novel homeodomain only protein-binding partner, induces skeletal muscle differentiation. J Biol Chem 2007; 282: 7700-7709.
[37] Banerji V and Gibson SB. Targeting metabolism and autophagy in the context of haematologic malignancies. Int J Cell Biol 2012; 2012: 595976.
[38] Dow CA, Lincenberg GM, Greiner JJ, Stauffer BL and DeSouza CA. Endothelial vasodilator function in normal-weight adults with metabolic syndrome. Appl Physiol Nutr Metab 2016; 41: 1013-1017.
[39] Xu Y. Transcriptional regulation of endothelial dysfunction in atherosclerosis: an epigenetic perspective. J Biomed Res 2014; 28: 47-52.
[40] Sena CM, Pereira AM and Seiça R. Endothelial dysfunction - a major mediator of diabetic vascular disease. Biochim Biophys Acta 2013; 1832: 2216-2231.
[41] Zhuhua Z, Zhiquan W, Zhen Y, Yixin N, Weiwei Z, Xiaoyong L, Yueming L, Hongmei Z, Li Q and Qing S. A novel mice model of metabolic syndrome: the high-fat-high-fructose diet-fed ICR mice. Exp Anim 2015; 64: 435-442.
[42] Poudyal H, Panchal S and Brown L. Comparison of purple carrot juice and β-carotene in a high-carbohydrate, high-fat diet-fed rat model of the metabolic syndrome. Br J Nutr 2010; 104: 1322-1332.

[43] Wada T, Kenmochi H, Miyashita Y, Sasaki M, Ojima M, Sasahara M, Koya D, Tsuneki H and Sasaoka T. Spironolactone improves glucose and lipid metabolism by ameliorating hepatic steatosis and inflammation and suppressing enhanced gluconeogenesis induced by high-fat and high-fructose diet. Endocrinology 2010; 151: 2040-2049.
[44] Chidambaram J and Carani Venkatraman A. Cissus quadrangularis stem alleviates insulin resistance, oxidative injury and fatty liver disease in rats fed high fat plus fructose diet. Food Chem Toxicol 2010; 48: 2021-2029.
[45] Lehnen AM, Rodrigues B, Irigoyen MC, De Angelis K and Schaan BD. Cardiovascular changes in animal models of metabolic syndrome. J Diabetes Res 2013; 2013: 761314.
[46] Li T, Lu X, Sun Y and Yang X. Effects of spinach nitrate on insulin resistance, endothelial dysfunction markers and inflammation in mice with high-fat and high-fructose consumption. Food Nutr Res 2016; 60: 32010.
[47] Miles JM, Wooldridge D, Grellner WJ, Windsor S, Isley WL, Klein S and Harris WS. Nocturnal and postprandial free fatty acid kinetics in normal and type 2 diabetic subjects: effects of insulin sensitization therapy. Diabetes 2003; 52: 675-681.
[48] Lu Y, Qian L, Zhang Q, Chen B, Gui L, Huang D, Chen G and Chen L. Palmitate induces apoptosis in mouse aortic endothelial cells and endothelial dysfunction in mice fed high-calorie and high-cholesterol diets. Life Sci 2013; 92: 1165-1173.
[49] Titov VN. The excess of palmitic fatty acid in food as main cause of lipoidosis of insulin-dependent cells: Skeletal myocytes, cardio-myocytes, periportal hepatocytes, kupffer macrophages and b-cells of pancreas. Klin Lab Diagn 2016; 61: 68-77.
[50] Aylett CH, Sauer E, Imseng S, Boehringer D, Hall MN, Ban N and Maier T. Architecture of human mTOR complex 1. Science 2016; 351: 48-52.
[51] Makki K, Taront S, Molendi-Coste O, Bouchaert E, Neve B, Eury E, Lobbens S, Labalette M, Duez H, Staels B, Dombrowicz D, Froguel P and Wolowczuk I. Beneficial metabolic effects of rapamycin are associated with enhanced regulatory cells in diet-induced obese mice. PLoS One 2014; 9: e92684.
[52] Tianshu C, Congrong G, Zhiwei Z, Fei L, Ayu S, Yuanbiao Z, Jing C and Ge J. Rapamycin combined with α-cyanoacrylate contributes to inhibiting intimal hyperplasia in rat models. Arq Bras Cardiol 2019; 112: 3-10.
[53] Ceylan-Isik AF, Dong M, Zhang Y, Dong F, Turdi S, Nair S, Yanagisawa M and Ren J. Cardiomyocyte-specific deletion of endothelin receptor A rescues aging-associated cardiac hypertrophy and contractile dysfunction: role of autophagy. Basic Res Cardiol 2013; 108: 335-63.
[54] Chambers metabolic syndrome, Rugo HS, Litton JK and Meiller TF. Stomatitis associated with mammalian target of rapamycin inhibition: a review of pathogenesis, prevention, treatment, and clinical implications for oral practice in metastatic breast cancer. J Am Dent Assoc 2018; 149: 291-298.
[55] Hahn D, Hodson EM, Hamiwka LA, Lee VW, Chapman JR, Craig JC and Webster AC. Target of rapamycin inhibitors (TOR-I; sirolimus and everolimus) for primary immunosuppression in kidney transplant recipients. Cochrane Database Syst Rev 2019; 12: Cd004290.
[56] Lloberas N, Cruzado JM, Franquesa M, Herrero-Fresneda I, Torras J, Alperovich G, Rama I, Vidal A and Grinyó JM. Mammalian target of rapamycin pathway blockade slows progression of diabetic kidney disease in rats. J Am Soc Nephrol 2006; 17: 1395-1404.
[57] Yang Y, Wang J, Qin L, Shou Z, Zhao J, Wang H, Chen Y and Chen J. Rapamycin prevents early steps of the development of diabetic nephropathy in rats. Am J Nephrol 2007; 27: 495-502.
[58] Kolosova NG, Muraleva NA, Zhdankina AA, Stefanova NA, Fursova AZ and Blagosklonny MV. Prevention of age-related macular degeneration-like retinopathy by rapamycin in rats. Am J Pathol 2012; 181: 472-477.
[59] Das A, Durrant D, Koka S, Salloum FN, Xi L and Kukreja RC. Mammalian target of rapamycin (mTOR) inhibition with rapamycin improves cardiac function in type 2 diabetic mice: potential role of attenuated oxidative stress and altered contractile protein expression. J Biol Chem 2014; 289: 4145-4160.
[60] Reifsnyder PC, Doty R and Harrison DE. rapamycin ameliorates nephropathy despite elevating hyperglycemia in a polygenic mouse model of type 2 diabetes, NONcNZO10/LtJ. PLoS One 2014; 9: e114324.
[61] Wang S, Zhou SL, Min FY, Ma JJ, Shi XJ, Bereczki E and Wu J. mTOR-mediated hyperphosphorylation of tau in the hippocampus is involved in cognitive deficits in streptozotocin-induced diabetic mice. Metab Brain Dis 2014; 29: 729-736.
[62] Gong FH, Ye YN, Li JM, Zhao HY and Li XK. Rapamycin-ameliorated diabetic symptoms involved in increasing adiponectin expression in diabetic mice on a high-fat diet. Kaohsiung J Med Sci 2017; 33: 321-326.
[63] Hartford CM and Ratain MJ. Rapamycin: something old, something new, sometimes borrowed and now renewed. Clin Pharmacol Ther 2007; 82: 381-388.

[64] Guo F, Li X, Peng J, Tang Y, Yang Q, Liu L, Wang Z, Jiang Z, Xiao M, Ni C, Chen R, Wei D and Wang GX. Autophagy regulates vascular endothelial cell eNOS and ET-1 expression induced by laminar shear stress in an ex vivo perfused system. Ann Biomed Eng 2014; 42: 1978-1988.
[65] DeMartino GN. Introduction to the thematic minireview series: autophagy. J Biol Chem 2018; 293: 5384-5385.
[66] Xie K, Jin B, Li Y, Luo X, Zhu J, Ma D and Shi H. Modulating autophagy improves cardiac function in a rat model of early-stage dilated cardiomyopathy. Cardiology 2013; 125: 60-68.
[67] Maejima Y. The critical role of autophagy in heart failure. Nihon Yakurigaku Zasshi 2018; 151: 100-105.
[68] Yan S and Xiu-ru G. Autophagy: a new target for the treatment of atherosclerosis. Frontiers in Laboratory Medicine 2018; S2542364-918300487.
[69] Lin XL, Xiao WJ, Xiao LL and Liu MH. Molecular mechanisms of autophagy in cardiac ischemia/reperfusion injury (Review). Mol Med Rep 2018; 18: 675-683.
[70] Kuroki T, Isshiki K and King GL. Oxidative stress: the lead or supporting actor in the pathogenesis of diabetic complications. J Am Soc Nephrol 2003; 14: S216-220.
[71] Zheng XT, Wu ZH, Wei Y, Dai JJ, Yu GF, Yuan F and Ye LC. Induction of autophagy by salidroside through the AMPK-mTOR pathway protects vascular endothelial cells from oxidative stress-induced apoptosis. Mol Cell Biochem 2017; 425: 125-138.
[72] Liu J, Wu J, Sun A, Sun Y, Yu X, Liu N, Dong S, Yang F, Zhang L, Zhong X, Xu C, Lu F and Zhang W. Hydrogen sulfide decreases high glucose/palmitate-induced autophagy in endothelial cells by the Nrf2-ROS-AMPK signaling pathway. Cell Biosci 2016; 6: 33-50.
[73] Chen P, Liu H, Xiang H, Zhou J, Zeng Z, Chen R, Zhao S, Xiao J, Shu Z, Chen S and Lu H. Palmitic acid-induced autophagy increases reactive oxygen species via the Ca(2+)/PKCα/NOX4 pathway and impairs endothelial function in human umbilical vein endothelial cells. Exp Ther Med 2019; 17: 2425-2432.
[74] Ye M, Qiu H, Cao Y, Zhang M, Mi Y, Yu J and Wang C. Curcumin Improves palmitate-induced insulin resistance in human umbilical vein endothelial cells by maintaining proteostasis in endoplasmic reticulum. Front Pharmacol 2017; 8: 148-60.
[75] Han J, Pan XY, Xu Y, Xiao Y, An Y, Tie L, Pan Y and Li XJ. Curcumin induces autophagy to protect vascular endothelial cell survival from oxidative stress damage. Autophagy 2012; 8: 812-825.
[76] Song J, Huang Y, Zheng W, Yan J, Cheng M, Zhao R, Chen L, Hu C and Jia W. Resveratrol reduces intracellular reactive oxygen species levels by inducing autophagy through the AMPK-mTOR pathway. Front Med 2018; 12: 697-706.
[77] Zhou X, Yang J, Zhou M, Zhang Y, Liu Y, Hou P, Zeng X, Yi L and Mi M. Resveratrol attenuates endothelial oxidative injury by inducing autophagy via the activation of transcription factor EB. Nutr Metab (Lond) 2019; 16: 42-54.
[78] Geng FH, Li GH, Zhang X, Zhang P, Dong MQ, Zhao ZJ, Zhang Y, Dong L and Gao F. Berberine improves mesenteric artery insulin sensitivity through up-regulating insulin receptor-mediated signalling in diabetic rats. Br J Pharmacol 2016; 173: 1569-1579.
[79] Cheraghi O, Abdollahpourasl M, Rezabakhsh A and Rahbarghazi R. Distinct effects of royal jelly on human endothelial cells under high glucose condition. Iran J Pharm Res 2018; 17: 1361-1370.
[80] Zhao Q, Yang H, Liu F, Luo J, Zhao Q, Li X and Yang Y. Naringenin exerts cardiovascular protective effect in a palmitate-induced human umbilical vein endothelial cell injury model via autophagy flux improvement. Mol Nutr Food Res 2019; 63: e1900601.
[81] Wirth M, Joachim J and Tooze SA. Autophagosome formation--the role of ULK1 and Beclin1-PI3KC3 complexes in setting the stage. Semin Cancer Biol 2013; 23: 301-309.
[82] Mizushima N, Yamamoto A, Hatano M, Kobayashi Y, Kabeya Y, Suzuki K, Tokuhisa T, Ohsumi Y and Yoshimori T. Dissection of autophagosome formation using Apg5-deficient mouse embryonic stem cells. J Cell Biol 2001; 152: 657-668.
[83] Itakura E, Kishi-Itakura C and Mizushima N. The hairpin-type tail-anchored SNARE syntaxin 17 targets to autophagosomes for fusion with endosomes/lysosomes. Cell 2012; 151: 1256-1269.
[84] Hebbachi A and Saggerson D. Acute regulation of 5'-AMP-activated protein kinase by long-chain fatty acid, glucose and insulin in rat primary adipocytes. Biosci Rep 2012; 33: 71-82.
[85] Ding WX. Uncoupling AMPK from autophagy: a foe that hinders the beneficial effects of metformin treatment on metabolic syndrome-associated atherosclerosis? Focus on "glucose and palmitate uncouple AMPK from autophagy in human aortic endothelial cells". Am J Physiol Cell Physiol 2015; 308: C246-248.